Available online at www.sciencedirect.com
SCIENCE DIRECT
International Journal of Pharmaceutics 317 (2006) 47–53
INTERNATIONAL JOURNAL OF PHARMACEUTICS
www.elsevier.com/locate/ijpharm

The effect of crystal imperfections on particle fracture behaviour

Onno de Vegt [a,*], Herman Vromans [a,b], Wim Pries [c], Kees van der Voort Maarschalk [a,d]

[a] *Department of Pharmaceutics, N.V. Organon, P.O. Box 20, 5340 BH Oss, The Netherlands*
[b] *Department of Pharmacy and Pharmaceutical Technology, University of Utrecht, The Netherlands*
[c] *Akzo Nobel, Powder Technology Department, Deventer, The Netherlands*
[d] *Department of Pharmaceutical Technology and Biopharmacy, University of Groningen, Groningen, The Netherlands*

Received 28 October 2005; received in revised form 22 February 2006; accepted 28 February 2006
Available online 4 April 2006

Abstract

Micronisation of active pharmaceutical ingredients is a process which is sometimes difficult to control. The main purpose of this study was to assess the effect of the pre-existing flaws in the material to be milled. The rate of breakage of four samples of a model compound (sodium chloride), originating from different sources, was determined in a jet mill. It appeared that each type of sodium chloride has a distinct particle rate of breakage and breakage pattern. The numbers of flaws in the different types of sodium chloride have been determined by immersing the sodium chloride particles in a liquid with the same refractive index. This makes the cracks better visible. Microphotographs were made and flaws were counted manually.

The study shows that the flaw density has an impact on the fracture behaviour of particles. The degree of fracture tends to increase with increasing flaw density. The paper shows however that the mechanical properties of the material as well as the starting particle size dominate the significance of the impact of flaws on fracture behaviour.

Keywords: Flaws; Milling; Micronisation; Particle rate of breakage; Particle size; Sodium chloride

1. Introduction

Crystallization is an important unit operation in the production of active pharmaceutical ingredients. One of the main purposes of crystallisation is the purification of the compound. However, crystallised particles always contain irregularities, such as impurities and dislocations. Product quality variations can occur depending on the specific crystallisation conditions used in the crystallisation process (Meadhra, 1995). Consequently, crystallisation kinetics can have an impact on crystal purity. The crystallisation kinetics determines the resulting particle size distribution, which is one of the main characteristics for product quality.

Active materials used in pharmaceutical product development are rarely ready for use as crystallised drug substance. Frequently, the particle size needs to be reduced. This can be required by the route of administration, e.g. pulmonal delivery. Another important reason for small particles is that the compound has a low solubility and dissolution rate, i.e. it is a class II (or IV) compound according to the biopharmaceutical classification system. In this case the specific surface area of a compound must be as high as possible in order to guarantee a sufficiently high bioavailability. There are several ways to make small particles but micronisation by (jet) milling is still preferred because of the high capacity and relatively low cost price.

Frequently, batch-to-batch variations in terms of particle size are encountered during milling, even when the same processing conditions are employed. Because milling conditions are kept constant, the conclusion is that alterations in particle properties must play a role. Cleary, the process lacks control which is an undesired situation because process control is essential. In addition, process control is a topic of increasing attention, for example via the process analytical technology initiative of the FDA.

During milling three basic types of material behaviour can be distinguished, i.e. elastic, elastic–plastic, and visco-elastic behaviour (Ward and Hadley, 1995). The particle fracture of a material in general depends on the crystalline structure of the

* Corresponding author. Tel.: +31 412 662342; fax: +31 412 662524.
E-mail address: onno.devegt@organon.com (O. de Vegt).

0378-5173/$ – see front matter © 2006 Elsevier B.V. All rights reserved.
doi:10.1016/j.ijpharm.2006.02.052

material to be milled, the processing conditions, and the pre-existing imperfections and flaws in the material (Rumpf, 1973). As far as we know, a quantitative characterisation of the effect of imperfections and flaws on particle fracture has not been performed. The aim of this paper is to investigate the importance of pre-existing flaws in the form of inclusions and impurities in the crystal lattice on particle fracture in order to improve control of the milling process.

2. Materials and methods

2.1. Material

Sodium chloride has been chosen as a model compound. Different sources and production methods give different inclusions in the form of vacuoles (that contain brine) and other lattice defects. However, the particle size and shape remain largely unchanged. Therefore, sodium chloride is a suitable model compound for this study. All materials used were produced by Akzo Nobel at different production areas: salt 1 from Stade (Germany), salt 2 from Hengelo (The Netherlands), an intermediate quality salt 3 Mariager (Denmark), and salt 4 from Stade which is chemically the purest salt.

Sodium chloride crystals are cubic in shape and were produced by evaporation of pickling brine saturated in natural rock salt. The internal moisture content of the salts was determined by heating a pre-determined amount of salt at a temperature of 710 °C for 1 h. The weight loss as a result of heating is the water content. Table 1 shows the particle size distribution of sodium chloride and the internal moisture contents of three of the four types of sodium chloride investigated.

2.2. Methods

2.2.1. Grinding

The milling experiments were performed in a 100 AFG fluidized bed opposed jet mill (Alpine, Augsburg, Germany). This kind of mill is specifically designed for continuous milling. To perform batch milling experiments the particle feed was closed and the classifier speed was set to the maximum speed (22 000 rpm) to limit the amount of fines leaving the mill chamber. Milling pressure was set at 5 bar which is a normal milling pressure for this type of mill. Experiments were performed by introducing 200 g of powder into the mill and turning on the milling gas for a given time period (20–80 s). For each experiment, the processing conditions were kept the same allowing differentiation between material properties. After milling, the whole powder content of the mill was removed for particle size analysis. Dry dispersion laser diffraction measurements were performed with a Malvern Instruments model Mastersizer 2000 (Malvern, UK). The Fraunhofer model was used for deconvolution of the diffraction pattern. The true density of sodium chloride was determined with a gas pycnometer (AccyPyc 1330, Micromeritics) using nitrogen as test gas.

Table 1
Particle size of sodium chloride and moisture content of the starting materials

Type	$D(v, 10\%)$ (μm)	$D(v, 50\%)$ (μm)	$D(v, 90\%)$ (μm)	Internal moisture (wt.%)
Salt 1	182	351	577	0.18
Salt 2	225	391	555	0.29
Salt 3	202	393	686	0.23
Salt 4	201	411	625	–

2.2.2. Determination of the number and length of flaws

A sample of about 10 g of material was hand sieved (ASTM standard sieves) into fractions, one fraction with particles smaller than 75 μm and one portion in the size range from 300 to 425 μm. To check for flaws, impurities and crystal defects, the salt crystals were immersed in benzaldehyde. Sodium chloride does not dissolve in this material but benzaldehyde has about the same refractive index (1.529, Lide, 2004) as sodium chloride (1.544, Lide, 2004). This makes the salt almost invisible, whereas flaws, impurities and crystal defects become better visible. The particles were investigated with an optical microscope (Jenaval, Zeiss, Jena, Germany). After focusing on the flaws at a certain level in the particle, a photograph was taken using a Sanyo CCD camera. Thereafter, the procedure was repeated for the next level, until photographs of all visible flaws and impurities present in the crystal were taken. The number of flaws and impurities were counted manually on each photo. Counting of the same flaw twice or more was prevented by comparing the photographs meticulously with each other. With this method it is possible to detect flaws in the x-direction as well as in the y-direction. However, it is impossible to determine the length of the flaws in the z-direction. Because of the cubic crystal lattice of sodium chloride the assumption is that there is no preferential orientation of the flaws. This means that determination of the flaw size in the xy plane represents the flaws in the entire volume and agrees with Weichert (1991). Due to the wavelength of visible light and the numerical aperture of the microscope, detection of flaws is restricted to flaws with a size larger than approximately 1 μm. Fig. 1 gives a schematic representation of the method.

3. Results and discussion

3.1. Rate of breakage function

The particle rate of breakage functions of all test materials have been determined. The particle rate of breakage function is the probability of a particle with a certain size to break per unit time. The rate of breakage function can be calculated using Kapur's approximation of the batch grinding equation (Kapur, 1970). The approach of Berthiaux and Dodds (1996) has been followed, that states that results can be described using only the first Kapur function. Fig. 2 shows the experimentally determined rate of breakage functions of the four types of sodium chloride crystals investigated.

Fig. 2 shows that the particle rate of fracture is a function of particle size. Furthermore, each type of sodium chloride shows a distinct particle rate of fracture behaviour. This difference is not explained by the variation in the experimental set-up, since

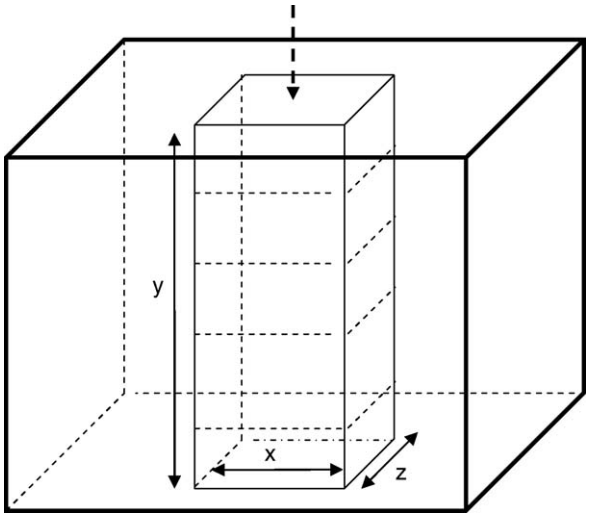

Fig. 1. Schematic representation of the arrangement to determine the number of flaws. The cube represents a particle where the number of flaws in a defined volume in the particle (represented by the interior) was determined at different levels. The dotted vertical arrow gives the viewing direction.

processing conditions were kept constant. Fig. 2 shows how fast the particles break. It is, however, also important to know the size of the fragments after fracture. This is the breakage distribution function. Berthiaux and Dodds (1996) showed that the breakage distribution function can be derived from the rate of breakage function (S):

$$b(i, j) = \frac{S_{i-1} - S_i}{S_j} \quad (1)$$

$b(i, j)$ is the fraction of broken product of size interval j which falls into size interval i. Fig. 3 shows the breakage distribution functions of particles of 555 μm of all salts.

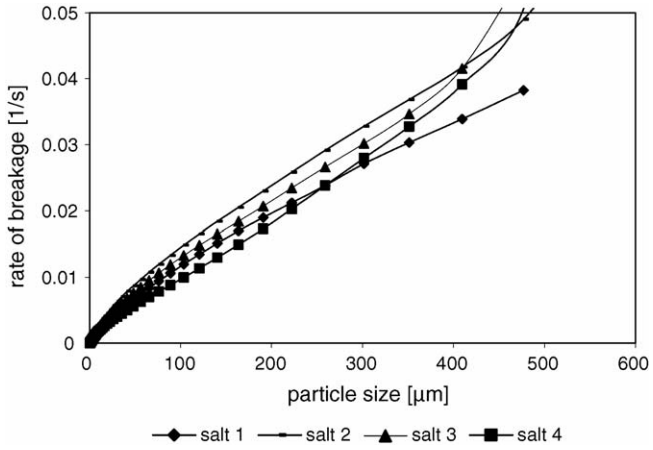

Fig. 2. Rate of breakage functions of sodium chloride. Processing conditions: 100 AFG mill, milling pressure 5 bar.

Fig. 3 shows that the different salt particles have distinct fracture patterns. Salt 4 breaks into some large fragments: 46% (by weight) of the broken fragments have a size of 477 μm (on average), just below the progeny particle size. These particles are the remainders of the original mother particles. The rest forms fragments consisting of particles with a size ranging from 0 to 477 μm. Fracture of salt 1 has a fracture pattern where the remaining mother particle becomes invisible. Salts 2 and 3 have intermediate properties.

Therefore, it is suggested that the observed differences in the particle rate of fracture (Fig. 2) and breakage distribution function (Fig. 3) are an effect of the differences in pre-existing flaws in the different types of sodium chloride crystals. This will be investigated in the next section.

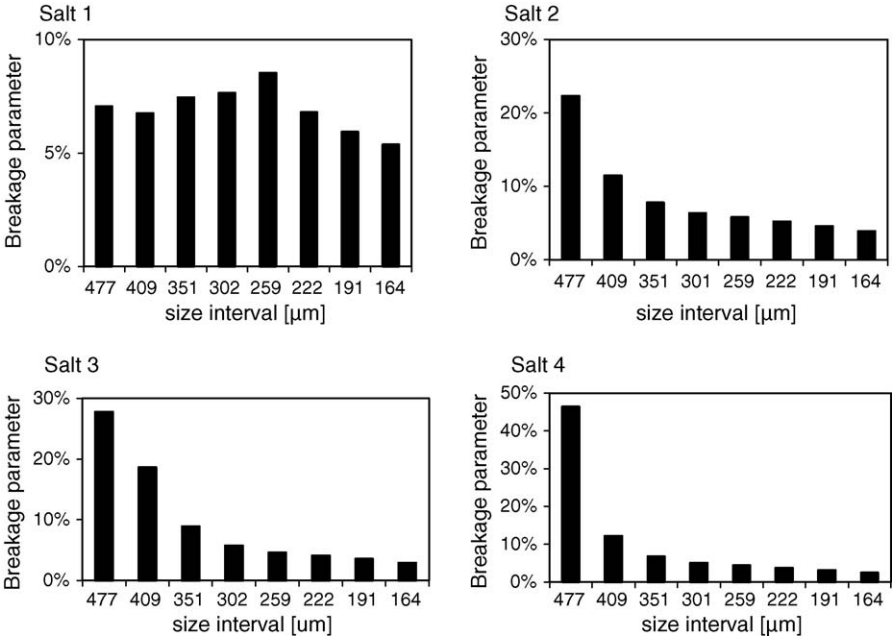

Fig. 3. Breakage distribution functions of sodium chloride particles with a size of 555 μm.

3.2. Assessment of breakage mechanism

Microscopic photographs have been taken of the different types of sodium chloride crystals studied before and after milling. Fig. 4 gives typical examples of the different salts.

The inclusions between the growth sectors in unmilled particles are clearly visible. Inclusions in the form of flaws can arise as an effect of several reasons. Sodium chloride is produced in multi stage crystallizers. During processing the crystals are subject to forces acting on them resulting in the formation of flaws. Whether the formation of cracks occurs or not depends mainly on the mechanical properties of the crystal and the loading conditions (Gahn and Mersmann, 1995). Furthermore, pre-existing flaws in a crystal can arise when during crystallization impurities are incorporated in the crystal.

At the corners and the edges a pile up of inclusions (dislocations) is seen, which is probably an effect of secondary nucleation (Meadhra, 1995). A visual comparison of the particles after

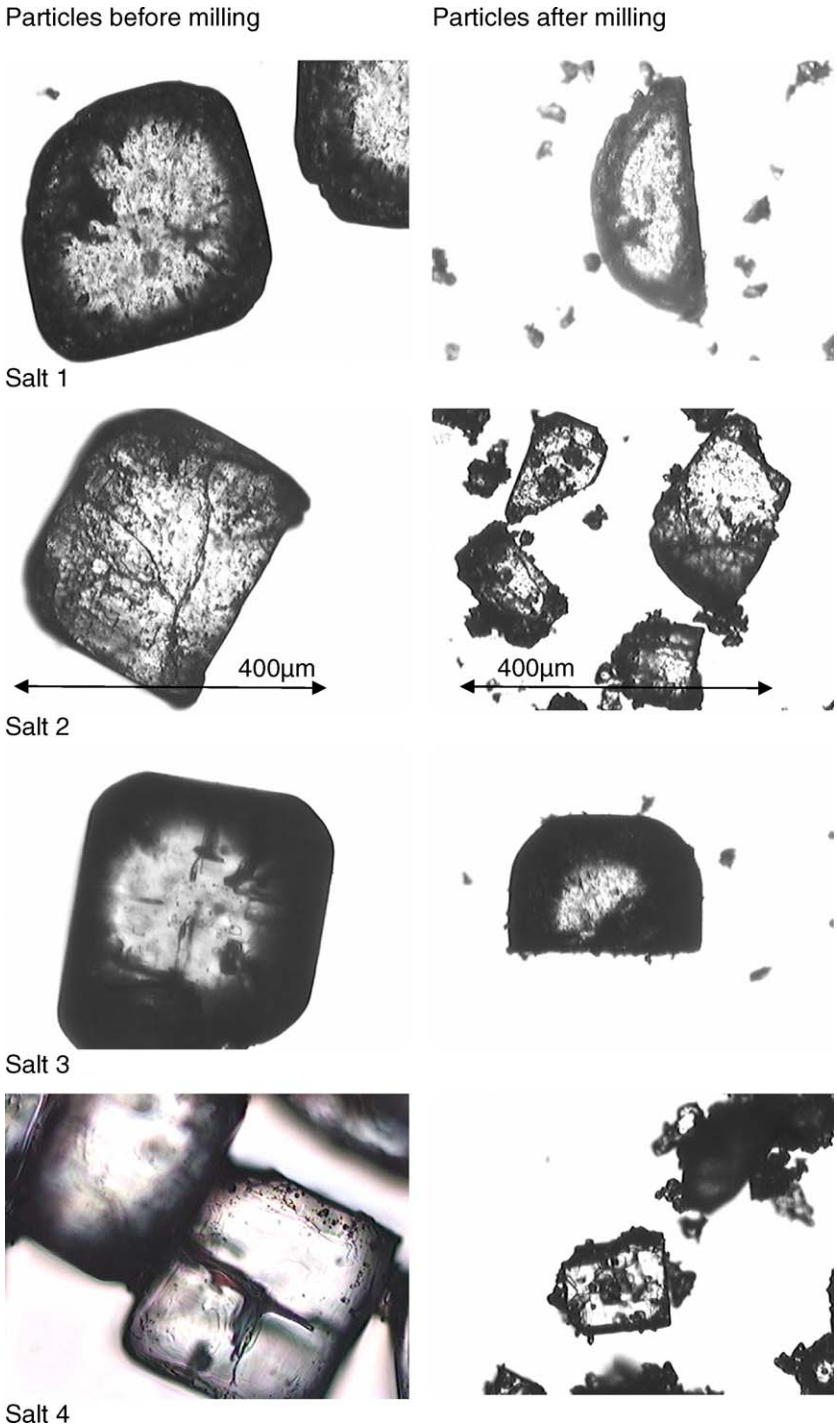

Fig. 4. Microscopic pictures of four different types of sodium chloride crystals before milling (left column) and after milling (right column). The unit scale corresponds to 400 μm and is valid for all pictures.

Table 2
Amount of flaws and the average flaw size of sodium chloride particles of different origins (particle size 362.5 μm)

Flaw size, l (μm)	Relative flaw size, l/x	Salt 1	Salt 2	Salt 3	Salt 4
3	0.0083	123	395	258	191
10	0.027	92	112	69	53
20	0.055	11	13	11	10
30	0.083	4	2	4	2
50	0.14	1	0	0	2
150	0.41	0	1	1	2
$\langle \ell \rangle$ (μm)		7.3	5.3	5.7	6.8
$\langle \ell \rangle / x$		0.020	0.014	0.016	0.019

milling and the breakage distribution functions (Fig. 3) suggests the same trends, albeit that it is very difficult to make a proper comparison.

Following the discussion of Bravi et al. (2003), brittle fracture occurs when the conditions for crack initiation are fulfilled. The main condition for that is the presence of large pre-existing cracks which act as notches. Furthermore, it has been proposed that fracture occurs along preferential planes, possibly following the path of the pre-existing cracks (Bravi et al., 2003).

It has also been suggested by Ghadiri and Papadopoulos (1995) that if no large pre-existing cracks are present, brittle fracture occurs in the chipping mode due to the enhanced dislocation density at the corners of the crystals resulting in stress amplification at the corners. On the basis of this discussion, it should be possible to correlate the fracture patterns in Fig. 3 with the flaw patterns as indicated in Fig. 4. In order to determine this, the flaw density and flaw size distribution have been determined.

3.3. Flaw size distribution

The number of flaws in specific flaw size ranges has been determined for large and small particles. From these data the average flaw size and average flaw size relative to the particle size have been determined. Table 2 lists the values for the large particles (size range of 300–425 μm) and Table 3 shows the results for particles with a size smaller than 75 μm.

Tables 2 and 3 show that the average flaw size is almost equal for the different types of crystals. Additionally, the average flaw size of the small particles is about three times smaller than the average flaw size of the larger particles. However, the flaws in the small crystals are relatively large as is illustrated by the difference in average relative flaw length. Furthermore, the data clearly shows that small particles contain flaws up to a size of 4 μm whereas the larger particles sometimes contain flaws with a size up to about 40% (150 μm) of the crystal size. Such relatively large flaws have never been observed in small particles. Rumpf (1973) suggested that the relative flaw size of similar particles of different sizes is constant. The data in this paper reveal that this might not be entirely correct for this specific material: flaws are relatively large in small particles, but some large particles contain very large cracks which have never been seen in small particles.

Table 3
Average number of flaws in sodium chloride particles of different origins (particle size <75 μm)

Flaw size, l (μm)	Relative flaw size, l/x	Salt 1	Salt 2	Salt 3	Salt 4
1.5	0.04	20	16	17	24
3	0.08	1	4	7	2
4	0.11	3	0	4	4
$\langle \ell \rangle$ (μm)		1.87	1.80	1.95	1.93
$\langle \ell \rangle / x$		0.068	0.048	0.052	0.051

Table 4
Number of flaws of four types of sodium chloride particles (size 300–425 μm)

Average flaw size (μm)	Salt 1		Salt 2		Salt 3		Salt 4	
	Initial	$t = 20$ s	Initial	$t = 20$ s	Initial	$t = 20$ s	Initial	$t = 20$ s
3	123	392	395	588	258	336	191	179
10	92	59	112	64	69	56	53	28
20	11	12	13	7	11	15	10	9
40	4	3	2	0	4	5	1	2
>50	2	3	0	0	0	3	2	2
$\sum$	232	469	522	659	342	415	257	220

Milling time was 20 s and milling pressure 5 bar.

Table 4 gives the flaw sizes of materials that have been milled for a short period of time. A comparison with the (large) unmilled particles reveals that in general the amount of small flaws increases (except for salt 4). The increase in number of flaws corresponds with the findings of Shipway and Hutchings (1993).

It has been recognised that not only flaw size but also flaw density plays a role (Weichert, 1991). Therefore, flaw densities in the particles have also been determined.

3.4. Flaw density

The flaw density is defined as the total amount of flaws present per volume. The volume of a crystal with a diameter of 362.5 μm is about 1.4×10^{-11} m^3 whereas the crystal volume with a diameter of 75 μm is about 8.4×10^{-14} m^3. Table 5 shows the flaw densities of the different types of sodium chloride crystals.

The flaw density of small crystals is higher than that of the larger crystals. This is surprising. Following the discussion of Rumpf (1973) a particle size independent flaw density is to be expected, but these data indicate that there is a particle size effect. Should a particle size effect be expected, then intuitively, it would be reasonable to expect that the large particles are relatively rich in flaws. It can be argued that the very large cracks in

Table 5
Flaw density of different types of sodium chloride crystals

Particle size (μm)	Flaw density (Flaws/m^3)			
	Salt 1	Salt 2	Salt 3	Salt 4
37.5	6.3×10^{14}	3.9×10^{14}	4.2×10^{14}	2.6×10^{14}
362.5	1.7×10^{13}	3.8×10^{13}	2.5×10^{13}	1.9×10^{13}

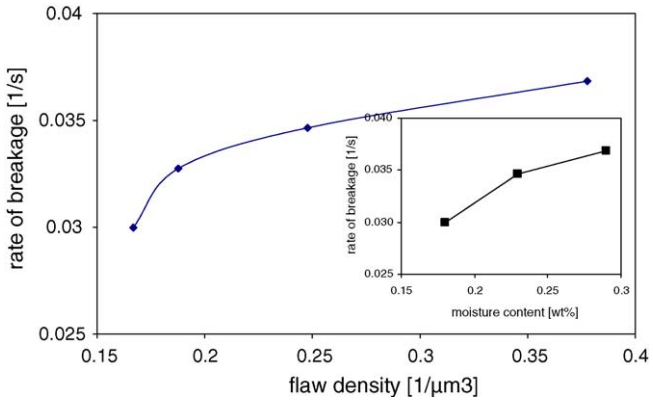

Fig. 5. Particle rate of breakage as a function of the flaw density in sodium chloride crystals. The inner graph shows the correlation between the rate of breakage and internal moisture content. Average crystal size is 362 μm.

the large particles (see Section 3.3) are the result of crack propagation via the small cracks. There is, however, no evidence for this suggestion.

The reciprocals of the values in Table 5 are the volumes in which one crack is present. When it is assumed that this volume is cubic, the average distance between cracks can be calculated. This distance is 10–13 μm for the small particles and 30–39 μm for the large ones. Kendall (1978) derived a relation to calculate the so-called brittle to ductile transition critical particle size. Particles larger than this size tend to deform brittle, while particles smaller than this size show a completely ductile deformation pattern. These small particles can only be deformed plastically and cannot be fractured at all, irrespective of the impact velocity (Ghadiri and Papadopoulos, 1995). For sodium chloride, this value was estimated to be 35 μm (Roberts et al., 1989). Interestingly, this value corresponds very well with the calculated inter-crack distance in the large sodium chloride particles.

Fig. 5 suggests that there is a relation between the particle rate of breakage and the flaw density of sodium chloride crystals with a size of 362 μm. A more practical method to determine flaw density is by measuring the internal moisture content of the salt particles, since these are correlated. The inner graph in Fig. 5 shows that there is a notable relationship between the rate of breakage and the internal moisture content in the different types of sodium chloride crystals.

The discussion so far indicates that there is an effect of flaw density on fracture behaviour. However, the flaw size may also have an effect on the fracture behaviour of the salt particles. Therefore, in the next section this effect has been investigated.

3.5. Relationship between the particle rate of fracture and average flaw size

Section 3.1 showed that each type of sodium chloride has a distinct particle rate of breakage, which also depends on particle size. In Section 3.3 the average flaw size of each type of salt is given. Fig. 6 correlates the particle rate of breakage and the average flaw size of sodium chloride crystals of two sizes, i.e. 35 and 351 μm.

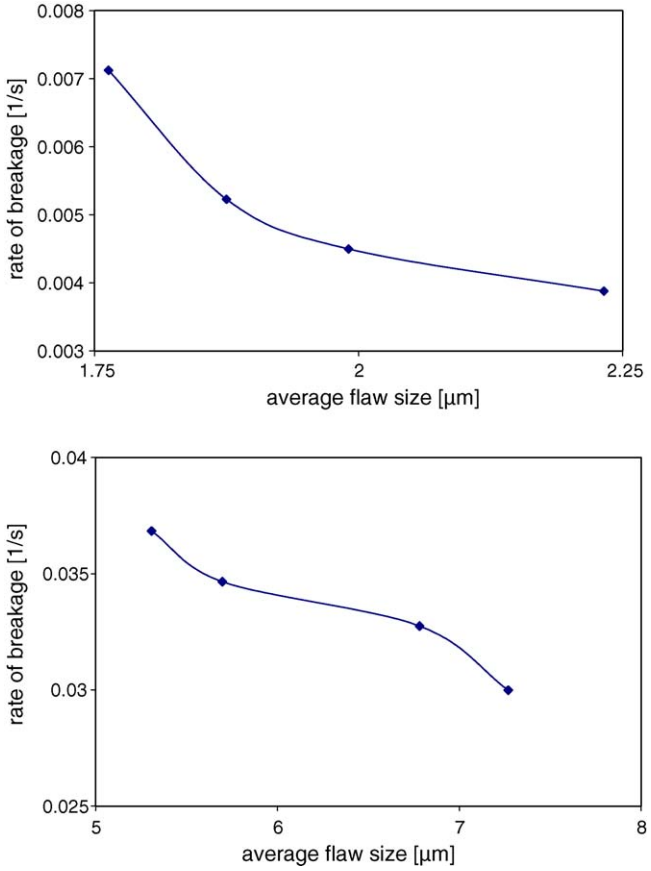

Fig. 6. Relationship between the particle rate of breakage and the average flaw size of flaws present in sodium chloride particles of two average particle sizes, i.e. 35 μm (upper figure) and 350 μm (lower figure). Crystals milled in a 100 AFG mill, milling pressure 5 bar.

Fig. 6 shows that the particle rate of breakage decreases with increasing average flaw size. This holds for both small and large particles. Tables 2 and 3 show that the salts with low average flaw size are rich in small flaws, i.e. a high flaw density is correlated with a small average flaw size. This implies that the (apparent) relation between rate of breakage and average flaw size is basically a relation between rate of breakage and flaw density. This agrees with conclusions from Weichert (1991) that state that crack propagation and branching occurs via the flaws present in the particle.

If a more plastic material would be milled the number of flaws generated would be less compared to the materials investigated in this study. This can be explained as follows. The more ionic, the crystals are likely to be less plastic and more easily deformed by brittle fracture. Pharmaceutical active materials have in general a soft (i.e. “weak”) crystal lattice. Soft crystals, those with great elasticity, will be more compliant and deform more readily since the intermolecular interactions are weaker than will stiffer crystals with large intermolecular potentials. However, the soft crystals will have a more homogenous distribution of the strain and will accommodate it more easily than the stiffer crystals can. Thus, the applied stress due to milling may be expected to generate more defects in the stiffer lattice than in the softer lattice that, although more greatly deformed, may have fewer defects

(Morris et al., 2001). Therefore, if a pharmaceutical active material would be milled, fewer defects would be generated in the crystal lattice resulting in a lower flaw density and hence, possibly in a lower rate of breakage.

4. Conclusions

In this study crystals of a model material, sodium chloride, from different sources have been tested on their fracture behaviours. The study shows that the size and density of flaws has an impact on the fracture behaviour of particles. The degree of fracture tends to increase with increasing flaw density. The paper also shows that the impact of particle size on fracture behaviour is larger. In a previous paper (Vegt et al., 2005), it has been clarified that the mechanical material properties are of eminent influence on the fracture behaviour. The paper shows however that the mechanical properties of the material as well as the starting particle size dominate the significance of the impact of flaws on fracture behaviour.

Acknowledgement

The contribution of D. Privitera, University of Rome, to the experimental work is gratefully acknowledged.

References

Berthiaux, H., Dodds, J.A., 1996. Approximate calculation of breakage parameters from batch grinding tests. Chem. Eng. Sci. 51, 4509.

Bravi, M., Di Cave, S., Mazzarotta, B., Verdone, N., 2003. Relating the attrition behaviour of crystals in a stirred vessel to their mechanical properties. Chem. Eng. J. 94, 223–229.

Ghadiri, M., Papadopoulos, D.G., 1995. Impact attrition of particulate solids. FRR 16-02.

Gahn, C., Mersmann, A., 1995. The brittleness of substances crystallized in industrial processes. Powder Technol. 85, 71–81.

Kapur, P.C., 1970. Kinetics of batch grinding. Part B. An approximate solution to the grinding equation. Trans. Soc. Min. Eng. AIME 247, 309.

Kendall, K., 1978. The impossibility of comminuting small particles by compression. Nature 272, 710–711.

Lide, D.R., 2004. CRC Handbook of Chemistry and Physics, 85th ed.

Meadhra, R.O., 1995. Modelling of the kinetics of suspension crystallizers. PhD Thesis. TU Delft.

Morris, K.R., Griesser, U.J., Eckhardt, C.J., Stowell, J.G., 2001. Theoretical approaches to physical transformations of active pharmaceutical ingredients during manufacturing processes. Adv. Drug Delivery Rev. 48, 91–114.

Roberts, R.J., Rowe, R.C., Kendall, K., 1989. Brittle-ductile transition in die compaction of sodium chloride. Chem. Eng. Sci. 44, 1647–1651.

Rumpf, H., 1973. Physical aspects of comminution and new formulations of a law of comminution. Powder Technol. 7, 145–159.

Shipway, P.H., Hutchings, I.M., 1993. Attrition of brittle spheres by fracture under compression and impact loading. Powder Technol. 76, 23–30.

Vegt, O.M., de Vromans, H., Faassen, F., Voort Maarschalk, K.V.D., 2005. Milling of organic solids in a jet mill. Part 1. Determination of the selection function and related. Mech. Mater. Prop. 22, 133–140.

Weichert, R., 1991. Theoretical prediction of energy consumption and particle size distribution in grinding and drilling of brittle materials. Part. Syst. Charact. 8, 55–62.

Ward, I.M., Hadley, D.W., 1995. An Introduction to the Mechanical Properties of Solid Polymers. John Wiley & Sons.